



Sources and characteristics of terrestrial carbon in Holocene-scale sediments of the East Siberian Sea

Kirsi Keskitalo¹, Tommaso Tesi^{1,3,4}, Lisa Bröder^{1,3}, August Andersson^{1,3}, Christof Pearce^{2,3}, Martin Sköld⁵,
Igor P. Semiletov^{6,7,8}, Oleg V. Dudarev^{7,8}, and Örjan Gustafsson^{1,3}

¹Department of Environmental Science and Analytical Chemistry, Stockholm University, 10691 Stockholm, Sweden

²Department of Geological Sciences, Stockholm University, 10691 Stockholm, Sweden

³Bolin Centre for Climate Research, Stockholm University, 10691 Stockholm, Sweden

⁴CNR-National Research Council of Italy, ISMAR-Marine Science Institute, 40129 Bologna, Italy

⁵Department of Mathematics, Stockholm University, 10691 Stockholm, Sweden

⁶International Arctic Research Center, University of Alaska Fairbanks, Fairbanks, AK 99775, USA

⁷Pacific Oceanological Institute, Russian Academy of Sciences, Vladivostok, 690041, Russia

⁸Tomsk Polytechnic University, Tomsk, 634050, Russia

Correspondence to: Örjan Gustafsson (orjan.gustafsson@aces.su.se)

Received: 17 February 2017 – Discussion started: 21 February 2017

Accepted: 16 August 2017 – Published: 22 September 2017

Abstract. Thawing of permafrost carbon (PF-C) due to climate warming can remobilise considerable amounts of terrestrial carbon from its long-term storage to the marine environment. PF-C can then be buried in sediments or remineralised to CO₂ with implications for the carbon–climate feedback. Studying historical sediment records during past natural climate changes can help us to understand the response of permafrost to current climate warming. In this study, two sediment cores collected from the East Siberian Sea were used to study terrestrial organic carbon sources, composition and degradation during the past ~ 9500 cal yrs BP. CuO-derived lignin and cutin products (i.e., compounds solely biosynthesised in terrestrial plants) combined with $\delta^{13}\text{C}$ suggest that there was a higher input of terrestrial organic carbon to the East Siberian Sea between ~ 9500 and 8200 cal yrs BP than in all later periods. This high input was likely caused by marine transgression and permafrost destabilisation in the early Holocene climatic optimum. Based on source apportionment modelling using dual-carbon isotope ($\Delta^{14}\text{C}$, $\delta^{13}\text{C}$) data, coastal erosion releasing old Pleistocene permafrost carbon was identified as a significant source of organic matter translocated to the East Siberian Sea during the Holocene.

1 Introduction

The amount of organic carbon (OC) stored in the northern circumpolar permafrost (PF) amounts to ~ 1300 Pg OC of which ~ 800 Pg OC is perennially frozen (the remaining 500 Pg is non-permafrost, seasonally thawing active-layer permafrost or talik; Hugelius et al., 2014). Northern Hemisphere circumpolar soils thereby hold roughly half of the global soil OC pool (Tamocai et al., 2009). Modelled future climate scenarios predict continued amplified warming in the Arctic for the coming 100 years (IPCC, 2013). This will further destabilise permafrost, leading to increased delivery of terrestrial OC to the Arctic Ocean. The potential decomposition of this relict permafrost carbon (PF-C) and its subsequent release to the atmosphere as CO₂ or CH₄ constitutes a positive feedback to global warming (IPCC, 2013; Koven et al., 2011; Schuur et al., 2015; Vonk and Gustafsson, 2013). Considering the size of the Arctic PF-C pool it is important to better understand the dynamics and extent of its vulnerability to remobilisation in response to climate warming.

Many recent studies have focused on current carbon cycling in the Arctic land–ocean continuum with possible linkages to climate change. Constraining how this system responded to earlier climate warming may help us to better predict the future response of PF-C and its climate couplings. The last glacial–interglacial transition constituted a major

climate rearrangement on Earth. The increase in mean temperature coupled with sea level rise is thought to have profoundly destabilised PF-C and further released CO₂ to the atmosphere (Ciais et al., 2013; Crichton et al., 2016; Köhler et al., 2014; Tesi et al., 2016a). Several studies have suggested that there was a warming-coupled translocation of terrestrial carbon during the climate warming that ended the latest glacial period (e.g., Bauch et al., 2001a; Ciais et al., 2013; Mueller-Lupp et al., 2000; Tesi et al., 2016a) similar to what is predicted to happen as a consequence of the anthropogenic climate change (Barnhart et al., 2014; Vonk and Gustafsson, 2013).

Many of the previous Holocene timescale studies in the East Siberian Arctic Shelf (ESAS) have focused on the Laptev Sea (e.g., Bauch et al., 2001b; Mueller-Lupp et al., 2000; Tesi et al., 2016a). This study focuses on the East Siberian Sea (ESS), which has not yet been extensively studied, especially for the historical reconstruction of PF-C dynamics. The ESS receives terrestrial OC by coastal erosion, fluvial inflow and possibly seabed erosion (Karlsson et al., 2016; Semiletov et al., 2005; Stein and Macdonald, 2004; Tesi et al., 2014, 2016b; Vonk et al., 2010). The coast of the ESS is dominated by carbon-rich Ice Complex deposits (ICD) consisting of old Pleistocene material (Schirrmeister et al., 2011; Semiletov, 1999a, b; Vonk et al., 2012). These large ICD bluffs are vulnerable to coastal erosion (Semiletov et al., 2013; Stein and Macdonald, 2004; Schirrmeister et al., 2011; Vonk et al., 2012). Coastal erosion can be further intensified with warming-enhanced processes like loss of sea ice cover, increasing frequency of storms, degradation of ice-bonded coasts and sea level rise (Barnhart et al., 2014; Jones et al., 2009; Stein and Macdonald, 2004). The largest rivers directly emptying into the ESS are Indigirka and Kolyma with suspended matter discharge of $11.1 \times 10^{12} \text{ g yr}^{-1}$ and $123 \pm 19 \times 10^9 \text{ g yr}^{-1}$ (Gordeev, 2006; McClelland et al., 2016, respectively) and an input also from the Lena River. The Lena River drains into the Laptev Sea, but its exported terrestrial OC is also transferred to the ESS via the Siberian Coastal Current (e.g., Alling et al., 2012; Sánchez-García et al., 2011). However, studies by Vonk et al. (2010, 2012) suggest that the contribution of ICD-PF erosion to the ESS sediment OC dominates over river discharge (ranging from 36 to 76 % in comparison to 5–35 %, respectively).

In this study we investigate land-to-ocean transfer and the fate of PF-C during the latest state of the post-glacial eustatic sea level rise until the present day. Our main objectives are to determine the sources and remobilisation fluxes of terrestrial OC and the composition and degradation status of the OC that was buried in ESS sediments during the Holocene. We characterise the OC composition by quantifying lignin phenols, cutin acids and other compounds yielded upon CuO oxidation to constrain the sources and degradation status of PF-C and the contribution of marine OC. Furthermore, we use a mixing model based on the isotopic composition ($\Delta^{14}\text{C}$, $\delta^{13}\text{C}$) of the deposited OC to quantify the con-

tribution of three different sources: topsoil-PF from active-layer deepening, ICD-PF and marine plankton. Additionally, we study how OC deposition fluxes have changed over time in response to the sea level rise and Holocene warming.

2 Materials and methods

2.1 Background and study area

The ESS is located off the northeastern Siberian coast between the Laptev Sea and the Chukchi Sea (Fig. 1). The ESS is one of the largest shelf seas ($987\,000 \text{ km}^2$) in the Arctic Ocean and one of the shallowest (mean depth 52 m; Jakobsen, 2002).

Thermokarst landscapes (i.e., thawing ice-rich permafrost) cover $\sim 20\%$ ($3.6 \times 10^6 \text{ km}^2$) of the northern circumpolar permafrost region (Olefeldt et al., 2016). Ice Complex deposit and thermokarst landscapes cover 2400 km of the ESS coastline (Grigoriev and Rachold, 2003). The modern average rate of coastal retreat in the ESS and the adjacent Laptev Sea is $1\text{--}10 \text{ m yr}^{-1}$ (Grigoriev, 2010), though even higher retreat rates (up to 24 and 30 m yr^{-1}) have been reported locally in the most actively eroding parts (Kanevskiy et al., 2016; Romanovskii et al., 2004). The coastal erosion rates have increased in the Arctic in recent decades (Barnhart et al., 2014; Günther et al., 2015; Jones et al., 2009). According to recent studies (Bröder et al., 2016b; Semiletov et al., 2013; Tesi et al., 2016b; Vonk et al., 2012), a large fraction of the remobilised PF-C is degraded during cross-shelf transport and released back to the contemporary carbon cycle. To better predict the consequences of the permafrost thaw, it is important to understand both the amount of remobilised organic carbon and its fate.

The shelf of the ESS contains terrestrial permafrost formed during the sea level low of the last glacial maximum (Jakobsen et al., 2014). During the Pleistocene–Holocene transition the ESAS was flooded when the sea level rose rapidly (Lambeck et al., 2014; Mueller-Lupp et al., 2000). This global marine transgression started $\sim 20\,000$ calyrs BP (Lambeck et al., 2014) and flooded the ESAS between $\sim 11\,000$ and $\sim 7\,000$ calyrs BP (Bauch et al., 2001a; Mueller-Lupp et al., 2000). The rate of the sea level rise was on the order of 1 cm yr^{-1} or more (Cronin et al., 2017; Stanford et al., 2011) in the early Holocene. The sampling site of the sediment core investigated in this study was flooded around 11 000 calyrs BP (Lambeck et al., 2014). The early Holocene temperatures in the Arctic regions were on average $1.6 \pm 0.8^\circ\text{C}$ higher than today (Kaufman et al., 2004) and the sea ice was at a low (Fisher et al., 2006).

Post-glacial sea level rise with warming and wetting of the climate caused a major relocation of permafrost carbon from land to the Arctic Ocean (Bauch et al., 2001a; Tesi et al., 2016a). Today the period when the ESS is only partially covered with sea ice is on average 3 months per year, which is one of the reasons why the area remains fairly unstud-

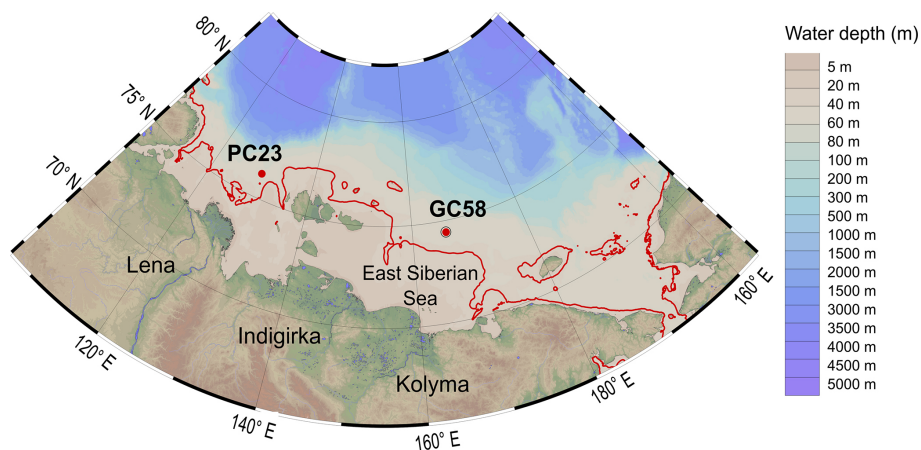


Figure 1. Map of the East Siberian Arctic Shelf showing the location of the sampling site (station SWERUS C3-1-58; Schlitzer, 2015). Also shown in the map is the location of the sediment core PC23 (station SWERUS C3-1-23; Tesi et al., 2016a). The red line marks the isobath (34 m of water depth), which is approximately where the coastline was at the beginning of the sediment archive (GC58) \sim 9500 cal yrs BP (Lambeck et al., 2014).

ied (Stein and Macdonald, 2004; Vetrov and Romankevich, 2004).

2.2 Sampling

A gravity core (called GC58) was collected in the ESS at 54 m of water depth as part of the international SWERUS-C3 research expedition on *I/B Oden* in August 2014. The coring site (Leg 1, station 58; 74.4387° N, 166.0467° E) is located \sim 500 km from the modern shoreline (Fig. 1). An additional sediment core was collected at the same site (MUC58) using a sediment multicorer (Oktopus GmbH, Germany), which is specifically designed to preserve the sediment–water interface. The total length of GC58 was 78 cm, while MUC58 was 32 cm long. The GC58 core was split in half during the expedition and kept refrigerated (+4 °C). In the laboratory at Stockholm University, one half was subsampled at 1 cm intervals and kept frozen at -18 °C. The multicore was sliced during the expedition at 1 cm intervals and then immediately frozen (-18 °C). Prior to analyses, the samples were freeze-dried at the Department of Environmental Science and Analytical Chemistry, Stockholm University, Sweden.

2.3 ^{210}Pb dating

Radiogenic ^{210}Pb was analysed with a gamma-ray spectrometer (GRS) at the Department of Geology of the Swedish Museum of Natural History in Stockholm, Sweden. The GRS determines the decay energy of radioisotopes in counts per second by measuring the gamma emission of the sample at a known energy level.

Prior to the GRS analysis, a subsample of approximately 10 g was homogenised and placed in a plastic container for at least 3 weeks to reach secular equilibrium between the radioisotopes of lead and radium (^{210}Pb and ^{226}Ra , respec-

tively). The samples were analysed for ^{210}Pb (46.51 keV), ^{226}Ra (186.05 keV) and ^{137}Cs (661.66 keV) on an EG&G Ortec[®] coaxial low-energy photon spectrometer containing a high-purity germanium detector. The counting period for each sample lasted 1–3 days depending on the amount of ^{210}Pb in the sample. An externally calibrated U-series standard (pitchblende; Stackebo, Sweden) was used to determine the relative efficiency of the gamma detector system. For each sample a minimum of 350 counts was acquired. A blank (empty container) sample was measured to correct for the background activity. The original method is described in detail by Elmquist et al. (2007).

Two different models were used for the ^{210}Pb dating: a CRS (constant rate of supply) model which assumes a constant rate of supply of excess ^{210}Pb fallout and a CIC (constant initial concentration) model which assumes a constant initial concentration of excess ^{210}Pb (Appleby and Oldfield, 1978).

2.4 Bayesian modelling of ^{14}C ages for the chronology

For the age–depth model construction, mollusc shells retrieved (hand-picked) from GC58 were analysed for their radiocarbon (^{14}C) content at the US NSF National Ocean Sciences Accelerator Mass Spectrometry (NOSAMS) facility at the Woods Hole Oceanographic Institution (WHOI; MA, USA). Prior to the analysis the mollusc shells were rinsed with MilliQ water and sonicated. The analysis followed standard procedures of NOSAMS (Pearson et al., 1998; Table 1).

To account for natural differences in the amount of ^{14}C in the atmosphere and differences between the marine environment and the atmosphere (e.g., Stuiver and Braziunas, 1993), all ^{14}C data were calibrated with the Marine13 calibration curve (Reimer et al., 2013). The offset in the local reservoir age was taken into account by using a ΔR of

Table 1. Radiocarbon (^{14}C) ages of the mollusc shells retrieved from the sediment core GC58. The ^{14}C ages are shown in years BP with an age error (yrs) and as calibrated ^{14}C ages (cal yrs BP) with 2 standard deviations ($\pm 2\sigma$) of the individual ^{14}C dates. The calibration curve used was Marine13 (Reimer et al., 2013) and a ΔR value of 50 ± 100 yrs (Bauch et al., 2001a). Also shown are the $\delta^{13}\text{C}$ (‰) values of the mollusc shells.

Corrected depth* (cm)	NOSAMS Accession no.	Type	Age ^{14}C (yrs BP)	Age error (yrs)	$\delta^{13}\text{C}$ (‰)	Age ^{14}C (Cal yrs BP) median	Age ^{14}C (Cal yrs BP) mean	2σ
3.5	OS-119395	Mollusc shell, fragments	895	25	0.55	462	455	184
8.5	OS-120688	Mollusc shell, fragments	> Modern	–	1.70	39	45	64
34.5	OS-120689	Mollusc shell, fragments	2260	20	1.55	1807	1806	250
39.5	OS-120690	Mollusc shell, fragments	2210	15	1.55	1748	1746	244
47.5	OS-123161	Mollusc shell, fragments	7960	35	0.90	8372	8372	220
51.5	OS-119396	Mollusc shell, fragments	8010	25	1.06	8426	8429	224
54.5	OS-120691	Mollusc shell, fragments	8020	20	0.49	8437	8441	226
65.5	OS-119397	Mollusc shell, <i>Macoma calcaria</i>	8780	25	−2.46	9384	9372	234
72.5	OS-120692	Mollusc shell, fragments	8880	20	−0.91	9493	9499	244
78.5	OS-120693	Mollusc shell, fragments	8950	25	−0.79	9579	9595	264

* Corrected depth is the original depth +3 cm to account for core top loss during sampling (Sect. 2.4).

50 ± 100 years. Since there are no ΔR values for the ESS in the literature, this ΔR value was taken from a study in the Laptev Sea (Bauch et al., 2001a). The radiocarbon dates are reported in calendar years before present (cal yrs BP; Stuiver and Polach, 1977).

The age model of the core was built with the OxCal v4.2 program based on the radiocarbon-dated mollusc shells and a depositional model (P_sequence, $k = 0.5$; Ramsey, 2008; Ramsey and Lee, 2013). Also, the base of the adjacent multicore dated with ^{210}Pb was used in the model. The ^{210}Pb date used was an average age (50 yrs BP) from the two ^{210}Pb dating models (CRS, CIC) for the bottom layer (12.5 cm) of the multicore (Table S2 in the Supplement). The age model of GC58 was constructed with a Bayesian statistics approach using the reservoir age (ΔR) and the depth as a prior model and measured radiocarbon dates as likelihoods. The posterior probability densities were acquired with a Markov chain Monte Carlo procedure which calculates possible distributions in order to date each sediment layer using the given prior model and likelihoods (Ramsey, 2008).

Sampling with a heavy gravity corer often disturbs the sediment–water interface and thereby causes losses of the surface sediments. The organic carbon (OC) content of GC58 was therefore compared to the OC content of the adjacent MUC58 to identify possible loss. According to the comparison, the top 3 cm was likely lost in GC58 (Fig. S1 in the Supplement) and thus corrected for.

2.5 Alkaline CuO oxidation

Microwave-assisted alkaline CuO oxidation was carried out using the method by Goñi and Montgomery (2000). Each homogenised subsample of around 300 mg was mixed with 300 mg of cupric oxide (CuO) and 50 mg of ammonium

iron (II) sulfate hexahydrate $((\text{NH}_4)_2\text{Fe}(\text{SO}_4)_2 \cdot 6\text{H}_2\text{O})$. After thorough mixing, nitrogen-purged 2M NaOH was added to each sample. Alkaline oxidation was performed with an UltraWAVE Milestone 215 microwave digestion system at 150°C for 90 min.

A known amount of internal recovery standards (ethylvanillin, cinnamic acid) was added to the CuO reaction products and then acidified to pH 1 with concentrated HCl (35 %). The CuO reaction products were repeatedly extracted using ethyl acetate (EtOAc). Anhydrous sodium sulfate (NaSO_4) was added to remove the remaining water. The extracts were dried in a CentriVap (Christ RVC 2-25) at 60°C , redissolved in pyridine and stored in a freezer (-18°C) until further analysis.

Finally, the samples were analysed with a gas chromatograph mass spectrometer (GC-MS; Agilent 7820A) using a DB5-MS capillary column (60 m \times 250 μm , 0.25 μm stationary phase thickness; Agilent J&W) at an initial temperature of 60°C followed by a ramp of 5°C min^{-1} until reaching 300°C . Prior to the GC-MS analysis, the extracts were derivatised with bis(trimethylsilyl)trifluoroacetamide (BSTFA) +1 % trimethylchlorosilane (TMCS) to silylate exchangeable hydrogens. The quantification of the samples was based on the comparison of the key ions to commercially available standards. Concentrations of CuO oxidation products were normalised to the organic carbon content of the sample and are reported as mg g^{-1} OC.

2.6 Bulk organic carbon and stable carbon isotope analyses

For the total organic carbon content (TOC), the total nitrogen content (TN) and the stable carbon isotope analysis ($\delta^{13}\text{C}$) of TOC, subsamples of 10–15 mg were homogenised and

placed in silver capsules, acidified with 1.5 M HCl to remove carbonates and then dried at 60 °C. The TOC, TN and $\delta^{13}\text{C}$ -TOC were quantified with an elemental analyser (Carlo Erba NC2500) connected via a split interface to a Finnigan MAT Delta V mass spectrometer at the Stable Isotope Laboratory of the Department of Geological Sciences at Stockholm University.

For radiocarbon (^{14}C) analysis of the bulk organic carbon, subsamples of sediment were acidified with 1.5 M HCl and sent to NOSAMS. To account for the time between the deposition and the measurement, the ^{14}C dates were calibrated with Eq. (1) using the age data derived from the age model. The bulk radiocarbon data are reported as $\Delta^{14}\text{C}$ (Stuiver and Polach, 1977):

$$\Delta^{14}\text{C} = (\text{Fm} \times e^{\lambda(1950-Y_c)} - 1) \times 1000, \quad (1)$$

where Fm is the fraction modern, λ is 1/mean life of radiocarbon = 1/8267 and Y_c is the year of collection derived from the age model (Stuiver and Polach, 1977).

2.7 Source apportionment

The carbon isotope fingerprint of OC ($\Delta^{14}\text{C}$, $\delta^{13}\text{C}$) can be used to quantitatively diagnose the relative contribution of topsoil-PF, ICD-PF and marine OC assuming isotopic mass balance (e.g., Vonk et al., 2012). In other words, the carbon isotopic signatures may help to understand whether the OC comes from coastal erosion as a result of the post-glacial warming and sea level rise, active-layer deepening of permafrost carbon in the watershed (as a response to the post-glacial warming) or sedimentation of marine phytoplankton. These different sources have a natural variability in their isotopic composition (endmembers). This variability needs to be taken into account to correctly estimate the relative source contributions and the associated uncertainties (e.g., Andersson, 2011). In previous studies a Bayesian Markov chain Monte Carlo (MCMC) approach has been used to estimate the relative source contributions for individual data points (Andersson et al., 2015; Tesi et al., 2016a). Here, we expand this approach to include the time dependence of the down-core isotopic signatures, taking advantage of the relatively small variability in the 78 $\delta^{13}\text{C}$ data points, whilst also using the 10 $\Delta^{14}\text{C}$ points. The time dependence of different proportions was taken into account by following the approach of Parnell et al. (2013). The method is described in detail in the ‘‘Supplementary methods’’ section in the Supplement.

The endmember values for the three source classes were taken from the literature (ICD-PF and topsoil-PF values compiled in Vonk et al., 2012; marine OC from Smith et al., 2002) for topsoil-PF ($\Delta^{14}\text{C} = -126 \pm 54 \text{‰}$, $\delta^{13}\text{C} = -28.2 \pm 1.96 \text{‰}$; mean \pm standard deviation) representing thaw of the active layer of permafrost, marine OC ($\Delta^{14}\text{C} = -60 \pm 60 \text{‰}$, $\delta^{13}\text{C} = -21 \pm 1 \text{‰}$) resulting from primary production of phytoplankton and ICD-PF ($\Delta^{14}\text{C} = -940 \pm$

84‰ , $\delta^{13}\text{C} = -26.3 \pm 0.63 \text{‰}$) resembling the old Pleistocene material from coastal erosion. The endmember value for ICD-PF was corrected with Eq. (1) to account for the age of the deposition.

2.8 Grain size analysis

Prior to the grain size analysis subsamples of sieved (500 μm) sediments from GC58 were homogenised. The grain size analysis was done with a Malvern Mastersizer 3000 laser diffraction particle size analyser, which can measure particles between 10 nm and 3.5 mm. Sodium hexametaphosphate (10 %) was used to disaggregate the particles suspended in deionised water. To further aid the disaggregation, all samples were exposed to ultrasound for 60 s and allowed to disperse in continuous flow for 3 min in total (including 60 s of ultrasonication) prior to the measurements. To control the concentration of the sample in the flow during the measurements, the obscuration was kept between 5 and 15 %. High sample obscuration (i.e., high concentration) would cause multiple light scatterings, thus distorting the results. Each sample was analysed in five replicates. The measurements were carried out at the Department of Geological Sciences at Stockholm University, Sweden.

3 Results and discussion

3.1 Age chronology of the core

The deepest part of the sediment core GC58 dates back to ~ 9500 cal yrs BP, i.e., to the early Holocene. The age-depth model shows an evident hiatus in the middle of the core between 39.5 and 40.5 cm resulting in an age gap of ~ 6500 years (~ 8200 – 1700 cal yrs BP; Fig. 2). In addition, there is a shorter gap in the chronology between ~ 9300 and ~ 8500 cal yrs BP. In studies from the adjacent Laptev Sea such age discrepancies have not been observed (Bauch et al., 2001a, b; Tesi et al., 2016a). It therefore seems likely that there has been a local event causing the removal of sediment layers. There might not have been accumulation during those periods, or the age gap could be a condensed unit of sediment. An actual sediment transport process giving rise to such a putative total halt in the sedimentation rate is rather elusive and unlikely. Since the whole ESAS is a very shallow shelf where sea ice is formed (Conlan et al., 1998; Jakobsson, 2002), another explanation for an age gap is ice scouring as observed in the Laptev Sea (Ananyev et al., 2016), especially at ~ 8500 cal yrs BP when the sea level was around 18 m lower (Lambeck et al., 2014) than today and the water depth at the coring site was around 32 m. At the time of the second age gap (~ 1700 cal yrs BP), the water depth at the coring site was approximately 52 m. An ice scouring event could have formed a gouge at the sea bottom that was later refilled with sediment (Barnes et al., 1984).

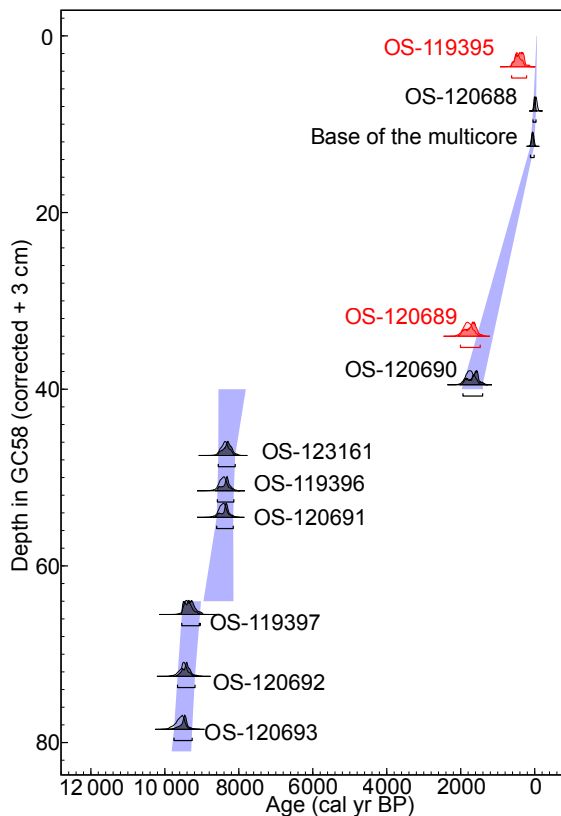


Figure 2. An age–depth model of the sediment core GC58 based on radiocarbon-dated (^{14}C) mollusc shells (see Table 1) and ^{210}Pb (base of a multicore collected at the same location; see Table S2 in the Supplement). All the modelled dates were calibrated with the Marine13 calibration curve (Reimer et al., 2013). A ΔR value of 50 ± 100 yrs was used to account for the differences in the local reservoir age based on Bauch et al. (2001a). The core GC58 dates back to ~ 9500 cal yrs BP. The calibrated age probability distributions are plotted for each radiocarbon date in grey. Outliers are coloured red. The blue shading indicates the modelled 2σ probability intervals for the entire depth range of the core, and the tiny black curves indicate 2σ for the individual measurements.

The accumulation rates of GC58 obtained from the ^{14}C measurements vary between 0.2 and 1.4 mm yr^{-1} (17.0 – $138.9 \text{ cm kyr}^{-1}$) and mass accumulation rates (MAR) spanned 0.02 – $0.1 \text{ g cm}^{-2} \text{ yr}^{-1}$. Bauch et al. (2001a) have reported similar sedimentation rates (0.1 – 2.6 mm yr^{-1}) from the outer shelf of the Laptev Sea around the same time period. The linear sedimentation rate for the adjacent sediment core MUC58 derived from ^{210}Pb dating is 1.3 mm yr^{-1} with an average MAR of $0.03 \text{ g cm}^{-2} \text{ yr}^{-1}$. Similar accumulation rates with ^{210}Pb -dated sediment cores have been reported in other studies from the ESS: 1.1 – 1.6 mm yr^{-1} (Vonk et al., 2012) and 1.4 – 1.5 mm yr^{-1} (Bröder et al., 2016a). The slight difference in accumulation rates using ^{210}Pb chronology compared to ^{14}C may be due to active biological mixing giving higher accumulation rates for the shorter timescale of

more surficial sediments (Baskaran et al., 2017; Boudreau, 1994).

3.2 Sediment grain size, stable carbon isotopes and biomarker composition of organic matter

Grain size can be used to describe the depositional environment. The sediment core GC58 consists mostly of clay and silt with a fraction of sand (Fig. S2 in the Supplement). The higher sand content that is observed at ~ 8500 cal yrs BP may reflect a higher-energy depositional regime likely due to preceding marine transgression and energetic coastal dynamics. Bauch et al. (2001a) have reported a shift from sandy silt to clayey silt around 7400 cal yrs BP from a sediment core collected in the eastern Laptev Sea. They attribute this change to the end of the sea level rise and the establishment of more stable conditions. The GC58 sediment core has a hiatus at that time period, but it has a similar clayey silt composition at the top part of the core (~ 1700 cal yrs BP until today). This may indicate comparably similar stable conditions in the ESS in the last 1700 cal yrs BP.

The total organic carbon (TOC) concentrations in GC58 vary from 0.5 to 1.1% (Table S1 in the Supplement) with the highest TOC content in the surface sediments. These data agree with average TOC contents reported for the ESS (Semiletov et al., 2005; Stein and Macdonald, 2004; Vetrov and Romankevich, 2004; Vonk et al., 2012). The OC fluxes for GC58 calculated with the ^{14}C age–model (covering ~ 9500 cal yrs BP) range between 1.2 and $10.9 \text{ g m}^{-2} \text{ yr}^{-1}$ (Fig. 3a). The OC fluxes for MUC58 calculated with the ^{210}Pb chronology (covering the most recent ~ 100 years) are similar and vary from 0.4 to $6.1 \text{ g m}^{-2} \text{ yr}^{-1}$ (Table S2 in the Supplement). The OC fluxes show an increasing trend from the bottom of the core toward the top in both cores. A similar trend has been reported by Bröder et al. (2016a) from the ESS using two ^{210}Pb -dated sediment cores. For GC58, the high OC flux at the very top of the core is likely related to the merging of the two dating systems (^{14}C and ^{210}Pb), which causes a higher sediment accumulation rate at the top of the core and thus higher fluxes.

Lignin phenols and cutin acids are useful proxies for tracing carbon of terrestrial origin because both compounds are solely biosynthesised in terrestrial plants. Lignin is an essential component in the cell walls of vascular plants (Higuchi, 1971), while cutin is a lipid polyester, which forms a protective wax layer on the epidermal cells of leaves and needles with other lipids (e.g., Kunst and Samuels, 2003). These compounds have been demonstrated to be useful in studying terrestrial OC in the Arctic (e.g., Amon et al., 2012; Bröder et al., 2016a; Goñi et al., 2013; Tesi et al., 2014). Both lignin and cutin fluxes show a similar trend with the highest fluxes at the bottom of the core (~ 9500 cal yrs BP) indicating a high proportion of terrestrial organic matter (Fig. 3b). The large variability in the fluxes between ~ 9500 and ~ 8200 cal yrs BP compared to the latest ~ 1700 cal yrs BP

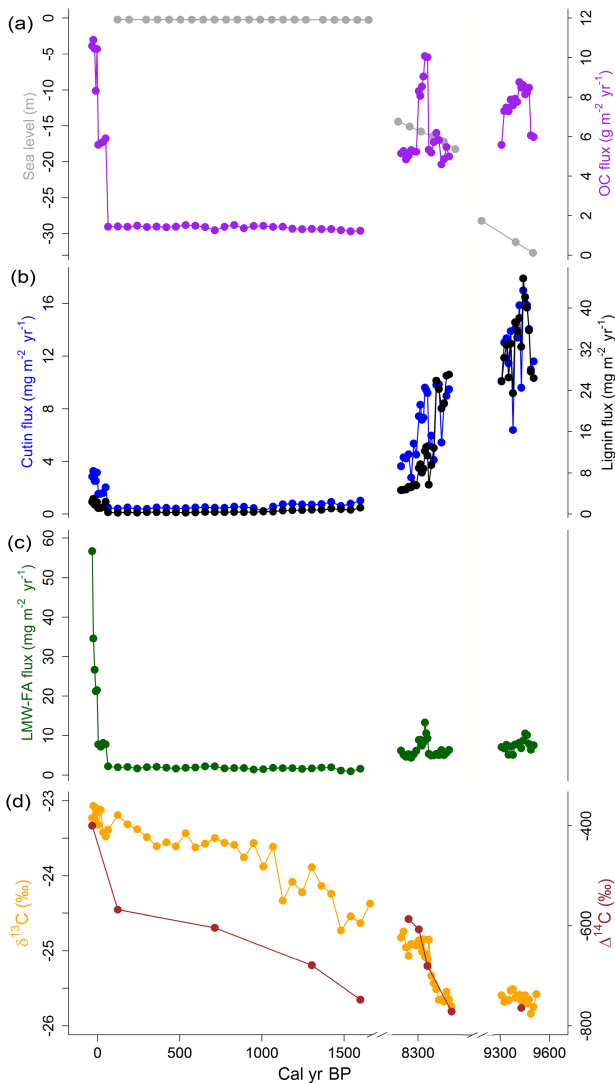


Figure 3. Organic matter composition of the sediment core GC58. The x axis has breaks due to gaps in the sediment chronology. **(a)** Organic carbon fluxes ($\text{g m}^{-2} \text{yr}^{-1}$) were high at the bottom of the core. The high fluxes at the top of the core are likely related to the merging of two dating systems (^{210}Pb and ^{14}C ; see Sect. 3.2). The sea level rose rapidly in the early Holocene (Lambeck et al., 2014). **(b)** Both lignin and cutin fluxes ($\text{mg m}^{-2} \text{yr}^{-1}$) decrease toward the core top. High fluxes at the top of the core are influenced by the OC fluxes and likely do not show an actual increase in the fluxes of lignin and cutin (see Sect. 3.2). **(c)** Low molecular weight fatty acids (LMW-FA) show an influence of marine organic matter at the top of the core. **(d)** The $\delta^{13}\text{C}$ (‰) values illustrate a gradual shift from terrestrial-dominated to more marine-dominated input of organic matter towards the core top. The $\Delta^{14}\text{C}$ (‰) values (corrected for the time between the deposition and the measurement) show that the bulk organic carbon is older at the bottom of the core than at the core top. The drop in the $\Delta^{14}\text{C}$ values ~ 1700 cal yrs BP is likely an artefact caused by the age model used to correct for the $\Delta^{14}\text{C}$ values.

suggests that the system was more dynamic at that time. The rapid decrease in both lignin and cutin fluxes indicates a change from terrestrially dominated to marine-dominated input at ~ 8400 cal yrs BP in this part of the ESS. Bauch et al. (2001b) suggested a similar regime shift from terrestrial to marine in the Laptev Sea between ~ 8900 and ~ 8400 cal yrs BP based on the occurrence of bivalves and benthic foraminiferal species. The same process affecting OC fluxes is likely also causing higher lignin and cutin fluxes at the top of GC58. The overall decrease in lignin and cutin fluxes as well as concentrations (Table S3 in the Supplement) in time is likely due to increasing hydrodynamic sorting and degradation during transport as transport times from the coast became longer because of the marine transgression (Fig. 3a). Bröder et al. (2016b) have observed a similarly strong decrease in the amount of terrestrial organic carbon depositions with increasing distance from the coast in the Laptev Sea. A recent study by Tesi et al. (2016b) shows that the largest particles, rich in lignin (i.e., plant debris), tend to be preferentially buried close to the shore with the cross-shelf transport of lignin occurring overwhelmingly bound to fine particles (with low settling velocities; i.e., of the total lignin deposited to the marine environment, only a fraction of $\sim 4\text{--}5\%$ travels across the shelf).

Other useful indicators of the marine input in organic matter are CuO-oxidation-derived low molecular weight fatty acids (LMW-FA). They are mainly found in phytoplankton but also in other organisms, such as bacteria and algae (Goñi and Hedges, 1995). C16FA:1 together with C14FA and C16FA serve as especially good proxies for marine OC as they are highly abundant in marine sediments and very low in concentrations in ICD-PF and topsoil-PF (Goñi and Hedges, 1995; Tesi et al., 2014). The highest fluxes of LMW-FA are observed for the very top of the core (Fig. 3c), indicating a larger proportion of marine OC. The values decrease rapidly down-core as marine FA are readily degraded (e.g., Bröder et al., 2016a; Canuel and Martens, 1996). This trend may also be influenced by the change in input from terrestrial- to marine-dominated sources.

The stable isotopic composition of bulk OC ($\delta^{13}\text{C}$) may be used to distinguish between marine and terrestrial organic matter (Fry and Sherr, 1984). The $\delta^{13}\text{C}$ values for C3-photosynthesised terrestrial carbon are between -23 and -30 ‰, whereas marine carbon has a less depleted $\delta^{13}\text{C}$ signature between -18 and 24 ‰ (e.g., Fry and Sherr, 1984). However, these endmember values may differ depending on the region, especially in the Arctic where open water and sea ice phytoplankton exhibit different isotopic fingerprints (Kohlbach et al., 2016). The $\delta^{13}\text{C}$ values for GC58 range from -23 to -25 ‰ (Fig. 3d) with the most depleted values (i.e., most terrestrial) between ~ 9500 and ~ 8200 cal yrs BP and the least depleted values (i.e., most marine) from ~ 1700 cal yrs BP until the modern time. Mueller-Lupp et al. (2000, and references within) have argued that $\delta^{13}\text{C}$ values in sediments of the Arctic Ocean can have a terrestrial

overprint in $\delta^{13}\text{C}$ composition caused by the rapid degradation of planktonic organic matter; i.e., the amount of marine organic matter in the total organic matter pool in the Arctic is relatively low. Yet, the gradual change in $\delta^{13}\text{C}$ indicates that the contribution of marine organic matter is greater at the top of the core where the $\delta^{13}\text{C}$ values are less depleted.

It is notable that the values for all the different parameters shown in Fig. 3 on both sides of the age gap (between ~ 8200 and ~ 1700 cal yrs BP) are nearly continuous in spite of the ~ 6500 year hiatus (except for the bulk $\Delta^{14}\text{C}$ OC values). Either the values actually are similar on both sides of the hiatus or, alternatively, this could be explained by bioturbation mixing the older part of the core with the newer deposits, thus resulting in an apparent continuity in property values across the hiatus. The $\Delta^{14}\text{C}$ values suggest that there was more ^{14}C -depleted material deposited at ~ 1600 cal yrs BP, causing a drop in the $\Delta^{14}\text{C}$ values. Though more likely, as the $\Delta^{14}\text{C}$ values are dependent on time, any uncertainty in the age model would have an effect on the $\Delta^{14}\text{C}$ values.

3.3 Degradation status of terrestrial organic matter

Lignin phenols provide insight into the degradation status of the deposited terrestrial organic matter. The acid to aldehyde, syringic acid to syringaldehyde (Sd / Sl) and vanillic acid to vanillin (Vd / Vl) ratios of lignin phenols have been used to study the degradation of lignin (e.g., Opsahl and Benner, 1995; Hedges et al., 1988). However, Goñi et al. (2000) and Tesi et al. (2014) have argued that the acid to aldehyde ratios of lignin phenols might not serve as a good degradation proxy for Arctic Ocean sediments as the material entering the marine environment might have experienced degradation prior to entering the marine system. This is supported by our data as both the Sd / Sl and Vd / Vl ratios show great variability throughout the core (Fig. S3 in the Supplement).

The ratio of 3,5-dihydrobenzoic acid to vanillyl phenols (3,5-Bd / V) is another proxy used to constrain the degradation status of terrestrial organic matter in sediments (e.g., Hedges et al., 1988; Tesi et al., 2014, 2016a). Specifically, this proxy is used to distinguish diagenetically altered mineral soil OC from relatively fresh vascular plant debris (Farella et al., 2001; Louchouart et al., 1999; Prahl et al., 1994). The only source of 3,5-Bd in the marine environment is brown algae, which are not common in the study area (Goñi and Hedges, 1995). The low 3,5-Bd / V ratio at the bottom of the core (~ 9500 – 8200 cal yrs BP) implies that the organic matter that was deposited in that period was relatively undegraded (Fig. S3 in the Supplement). The extent of degradation gradually increases toward the top of the core. However, hydrodynamic sorting may affect the degradation values as the largest particles of fresh vascular plant debris are likely buried close to the coast (Tesi et al., 2016b). The input of organic matter was higher before ~ 8200 cal yrs BP, presumably due to coastal erosion caused by the marine transgression. When sediments are quickly buried they can

serve as a more effective sink for terrestrial organic matter (Hilton et al., 2015). As the material is less degraded and the sedimentation rates are high in GC58 between ~ 9500 and ~ 8200 cal yrs BP, the input of organic matter was likely high causing it to be quickly buried. Similarly high input of terrestrial material has been observed in the Laptev Sea $\sim 11\,000$ cal yrs BP (Tesi et al., 2016a).

The location of the study site is currently ~ 500 km offshore so transport time and thereby the oxygen exposure time of the organic matter in the benthic compartment are now longer than in the earlier phase of the Holocene. The longer distance from the coast allows more time for organic matter to degrade before burial (Bröder et al., 2016b). Hartnett et al. (1998) have also shown that the burial efficiency of organic carbon decreases as a function of oxygen exposure time. The same trend can be seen in the fraction of remaining lignin ($f_{\text{lignin/terrOC}}$), i.e., the amount of lignin as a ratio of the observed and expected (assuming conservative mixing, i.e., no degradation) concentrations of lignin and terrestrial OC (terrOC; see “Supplementary methods” in the Supplement for details). In GC58 the $f_{\text{lignin/terrOC}}$ decreases down-core likely as a result of the preceding marine transgression (Fig. S4 in the Supplement). This trend suggests that with longer transport time the lignin degradation is more extensive due to the protracted oxygen exposure time and hydrodynamic sorting (Keil et al., 2004; Tesi et al., 2016a). We estimated this lateral transport time to be ~ 1.4 kyr longer at modern times than at the beginning of the Holocene for the station GC58 (Fig. S5 in the Supplement). To model the lateral transport times, we used $f_{\text{lignin/terrOC}}$ with individual degradation rates for terrOC and lignin (Bröder et al., 2015; see “Supplementary methods” in the Supplement).

3.4 Dual-isotope-based source apportionment of OC

The source apportionment results show that most of the organic matter originates from coastal erosion since ICD-PF material is the largest fraction (41–91 %) throughout the core (Fig. 4). Earlier studies demonstrated that the decay of fresh marine organic matter is more rapid compared to the degradation of terrestrial organic matter (Karlsson et al., 2011, 2015; Salvadó et al., 2016; Vonk et al., 2010). This may lead to the selective preservation of terrestrial organic matter in the sediments of the ESAS (Karlsson et al., 2011, 2015; Vonk et al., 2010). The contribution of topsoil-PF is fairly low throughout the core (3–23 %). This may be due to the location of GC58 between two major rivers (Kolyma and Indigirka), resulting in relatively low amounts of fluvial inflow depositing topsoil permafrost.

To further interpret our results within a larger context of PF-C destabilisation during post-glacial warming, we compared our results with another transgressive deposit collected in the Laptev Sea (PC23, Fig. 1; Tesi et al., 2016a). For the Laptev Sea (PC23), there was a predominant influence of watershed-sourced material via river discharge during the

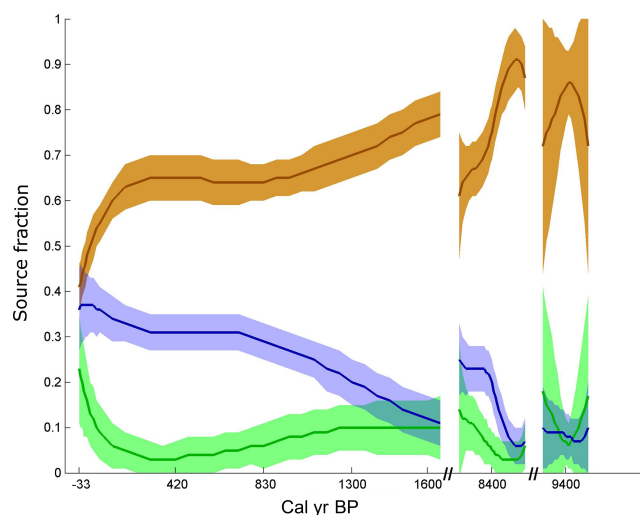


Figure 4. The dual-carbon-isotope-based ($\delta^{13}\text{C}$, $\Delta^{14}\text{C}$) source apportionment of organic carbon (OC) illustrates fractions (%) of old Pleistocene permafrost (ICD-PF) in brown, thaw of active-layer permafrost (topsoil-PF) in green and primary production (marine OC) in blue of the sediment core GC58. The ICD-PF is the dominant fraction throughout the core.

onset of the Holocene followed by similar contributions of marine OC and ICD-PF fractions (both sources varying between 31 and 56 %) from ~ 8300 calyrs BP to present. For the ESS (GC58), the contribution of ICD-PF is more prominent for the same time period, indicating a higher significance of coastal erosion for the ESS compared to the Laptev Sea (Fig. 5), especially when compared to the early Holocene signature. Topsoil-PF fractions in PC23 are slightly higher (8–25 %) than in GC58 (3–23 %) from ~ 8300 calyrs BP to current day. The difference is likely caused by a strong influence of the Lena River at the sampling location of PC23 and less fluvial inflow to GC58 due to its location farther away from the mouths of the Lena, Kolyma and Indigirka rivers.

When the shoreline was farther seaward during the early Holocene, the location of the core PC23 from the Laptev Sea experienced a large influence by material derived from the Lena River (80–90 %; Tesi et al., 2016a). This material was supplied to the Laptev Sea in response to the deglaciation and associated active-layer deepening in the watershed (Tesi et al., 2016a). Although the record of GC58 does not go back in time to the glacial–interglacial transition at the very onset of the Holocene, we suggest that coastal erosion was likely an important process affecting the permafrost carbon supply and deposition at that time. This seems possible, especially when considering the location of the core GC58 between the rivers and as has been observed in modern day shallower sediments in the ESS (Bröder et al., 2016a; Vonk et al., 2012).

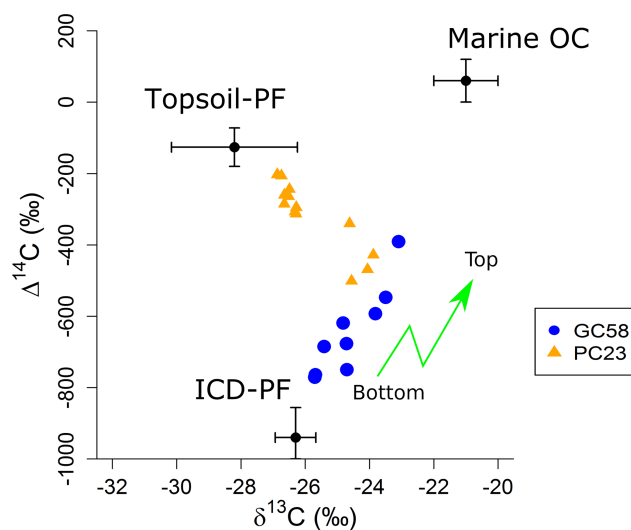


Figure 5. Dual-carbon isotope ($\delta^{13}\text{C}$, $\Delta^{14}\text{C}$) composition of the sediment cores GC58 (this study) and PC23 (Tesi et al., 2016a). Topsoil-PF refers to organic matter from the active layer of permafrost, ICD-PF to relict Pleistocene Ice Complex deposit permafrost (yedoma) and marine OC to organic matter from primary production. The endmember values for different sources are taken from a dataset compiled by Vonk et al. (2012) and a study by Smith et al. (2002). The green arrow points to the direction from the bottom to the top of the core (GC58).

3.5 Sources of terrestrial organic matter

The lignin fingerprint of organic matter sources in GC58 is consistent with the dual-carbon isotope modelling. Here we focus on the ratios of cinnamyl to vanillyl phenols and syringyl to vanillyl phenols (C/V and S/V, respectively). The C/V ratio can be used to differentiate between woody (i.e., shrubs and trees) and non-woody (i.e., leaves, needles, grasses) plant tissues as origins of terrestrial OC since cinnamyl phenols are produced only in non-woody vascular plant tissues (Hedges et al., 1988). Moreover, the S/V ratio differentiates between gymnosperms (conifers) and angiosperms (flowering plants) as syringyl phenols are produced solely in angiosperms (Hedges et al., 1988). Thereby higher S/V ratios mean more of a contribution from angiosperm plants.

The S/V and C/V ratios in GC58 show that the terrestrial material transported to the ESS originates mainly from soft tissue material (i.e., grasses and leaves) both from angiosperm and gymnosperm plants (Fig. 6). The lignin fingerprint of old Pleistocene material (ICD-PF) is characterised by high ratios of both C/V and S/V i.e., a high abundance of soft plant tissues from tundra steppe vegetation (e.g., grass-like material; Tesi et al., 2014; Winterfeld et al., 2015). Observations from the Laptev Sea (sediment core PC23, Fig. 1) reveal a much stronger influence from woody material indicating a watershed source, likely from the Lena River, rather than from coastal erosion (Fig. 6). It should be noted

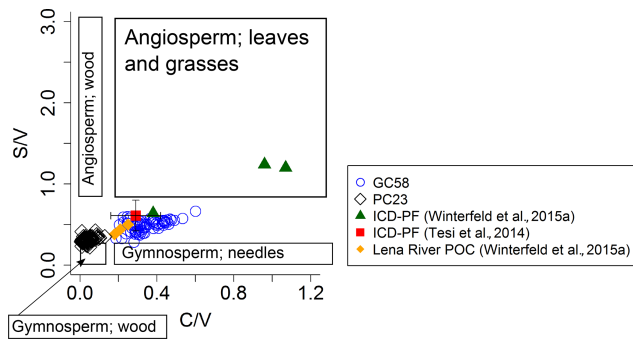


Figure 6. Lignin composition of the sediment core GC58 (blue circles). The ratio between cinnamyl and vanillyl phenols (C/V) is used as a proxy to distinguish between soft and woody plant tissues. The ratio of syringyl to vanillyl phenols (S/V) indicates the difference between gymnosperm and angiosperm plants. The boxes indicate the typical values for S/V and C/V ratios characterising different plant material (ranges from Goñi and Montgomery, 2000). Measured S/V and C/V ratios for Ice Complex deposit permafrost (ICD-PF) are shown with green triangles (Winterfeld et al., 2015) and with a red square (\pm standard deviation; Tesi et al., 2014). Measured S/V and C/V ratios for topsoil-PF (Lena River POC) are illustrated with orange diamonds (Winterfeld et al., 2015). Also shown is the lignin composition of the sediment core PC23 (black diamonds) from the Laptev Sea (study by Tesi et al., 2016a).

that the lignin phenols are susceptible to degradation. Cinnamyl phenols in particular are known to degrade fairly fast, which may lower the C/V ratios (Opsahl and Benner, 1995). However, even considering degradation effects, the relatively high C/V and S/V values that characterise GC58, indicate grass-type material typical of tundra and steppe biomes and ICD-PF deposits (Tesi et al., 2014; Winterfeld et al., 2015).

4 Conclusions

This down-core study provides new insights into terrestrial carbon dynamics in the ESS from the early Holocene warming period until the present. Our results suggest a high input of terrestrial organic carbon to the ESS during the last glacial–interglacial period caused by permafrost destabilisation. This material was mainly characterised as relict Pleistocene permafrost released via coastal erosion as a result of the sea level ingression.

The flux rates of both lignin and cutin compounds show a declining trend in the early Holocene, suggesting a change from mainly terrestrial- to marine-dominated input. The same change can be seen in the stable carbon isotope ($\delta^{13}C$) data, which imply a regime shift from terrestrial- to more marine-dominated sediment input at ~ 8400 cal yrs BP.

The source apportionment data highlight the importance of coastal erosion as a terrestrial carbon source to the ESS during the Holocene time periods of ~ 9500 – 9300 , ~ 8500 – 8200 and ~ 1700 cal yrs BP to the modern day. This is sup-

ported by the lignin composition, which suggests a deposition of tundra and steppe vegetation (i.e., grasses) grown during the Pleistocene. Both the biomarker and grain size data imply that the conditions have been more stable in the ESS in the past ~ 1700 cal yrs BP compared to the early Holocene.

The comparison of the source apportionment results ($\delta^{13}C$, $\Delta^{14}C$) and the lignin fingerprint (C/V and S/V ratios) for the sediment cores GC58 and PC23 shows a difference in the carbon sources between the ESS and the adjacent Laptev Sea. The relict Pleistocene permafrost, mostly originating from coastal erosion, may be more dominant in the ESS than in the Laptev Sea. Data for the sediment core PC23 show that the Laptev Sea instead had a relatively high input of terrestrial carbon from the watershed, which is likely due to the influence of the Lena River.

The accelerating coastal erosion rates along the Siberian coast and amplified warming in the Arctic predicted by many climate models are likely to cause permafrost destabilisation and remobilisation of terrestrial carbon to the marine environment, as observed at the beginning of the Holocene. To better understand the consequences of the permafrost thawing processes, the extent of degradation of terrestrial carbon in the marine environment should be better constrained. Also, to improve the understanding of the processes in the ESS and in the whole Arctic region, more historical down-core studies are needed.

Data availability. The data are available online in the Bolin Centre Database under the category “Marine” followed by “Arctic carbon”: <http://bolin.su.se/data/?c=marine>.

The Supplement related to this article is available online at <https://doi.org/10.5194/cp-13-1213-2017-supplement>.

Author contributions. TT and ÖG conceived and designed the research project. TT, LB, IS, OD and ÖG collected the samples with help from the *I/B Oden* crew. CP and KK developed the age–depth model of GC58. KK carried out all chemical and geological analyses on GC58 and MUC58. MS and AA ran the MCMC simulation for the OC source apportionment. AA estimated the lateral transport times. KK wrote the paper and produced the figures with input from all the co-authors.

Competing interests. The authors declare that they have no conflict of interest.

Special issue statement. This article is part of the special issue “Climate–carbon–cryosphere interactions in the East Siberian Arctic Ocean: past, present and future (TC/BG/CP/OS inter-journal SI)”. It is not associated with a conference.

Acknowledgements. We thank the crew and personnel of I/B *Oden*. We thank Rienk Smittenberg for the use of the microwave extraction facilities. We also thank Carina Jakobsson, Heike Siegmund and Karin Wallner for their help with the laboratory analyses at the Department of Geological Sciences at Stockholm University and at the Department of Geology of the Swedish Museum of Natural History. This study was supported by the Knut and Alice Wallenberg Foundation (KAW contract 2011.0027), the Swedish Research Council (VR contracts 621-2004-4039 and 621-2007-4631), the Nordic Council of Ministers Cryosphere–Climate–Carbon Initiative (project Defrost, contract 23001) and the European Research Council (ERC-AdG project CC-TOP no. 695331). Additionally, Igor P. Semiletov thanks the Russian Government for financial support (mega-grant under contract no. 14.Z50.31.0012). Oleg V. Dudarev thanks the Russian Science Foundation for financial support (no. 15-17-20032). Tommaso Tesi acknowledges EU financial support as a Marie Curie fellow (contract no. PIEF-GA-2011-300259); contribution no. 1916 of ISMAR-CNR Sede di Bologna. Lisa Bröder acknowledges financial support from the Climate Research School of the Bolin Centre for Climate Research. Christof Pearce received funding from the Danish Council for Independent Research/Natural Science (project DFF-4002-00098/FNU). Martin Sköld acknowledges financial support from the Swedish Research Council (grant 2013:05204). We also want to thank the editor, Thomas Cronin, and two anonymous reviewers for their insightful comments.

Edited by: Thomas M. Cronin

Reviewed by: Thomas M. Cronin and two anonymous referees

References

- Alling, V., Porcelli, D., Mörth, C. M., Anderson, L. G., Sanchez-Garcia, L., Gustafsson, Ö., Andersson, P. S., and Humborg, C.: Degradation of terrestrial organic carbon, primary production and out-gassing of CO₂ in the Laptev and East Siberian Seas as inferred from δ¹³C values of DIC, *Geochim. Cosmochim. Acta*, 95, 143–159, <https://doi.org/10.1016/j.gca.2012.07.028>, 2012.
- Amon, R. M. W., Rinehart, A. J., Duan, S., Louchouart, P., Prokushkin, A., Guggenberger, G., Bauch, D., Stedmon, C., Raymond, P. A., Holmes, R. M., McClelland, J. W., Peterson, B. J., Walker, S. A., and Zhulidov, A. V.: Dissolved organic matter sources in large Arctic rivers, *Geochim. Cosmochim. Acta*, 94, 217–237, <https://doi.org/10.1016/j.gca.2012.07.015>, 2012.
- Ananyev, R., Dmitrevskiy, N., Jakobsson, M., Lobkovsky, L., Nikiforov, S., Roslyakov, A., and Semiletov, I.: Sea-ice ploughmarks in the eastern Laptev Sea, East Siberian Arctic shelf, *Atlas Submar. Glacial Landforms Mod. Quat. Ancient, Geol. Soc. London, Mem.*, 46, 301–302, <https://doi.org/10.1144/M46.109>, 2016.
- Andersson, A.: A systematic examination of a random sampling strategy for source apportionment calculations, *Sci. Total Environ.*, 412–413, 232–238, <https://doi.org/10.1016/j.scitotenv.2011.10.031>, 2011.
- Andersson, A., Deng, J., Du, K., Zheng, M., Yan, C., Sköld, M., and Gustafsson, Ö.: Regionally-varying combustion sources of the January 2013 severe haze events over eastern China, *Environ. Sci. Technol.*, 49, 2038–2043, <https://doi.org/10.1021/es503855e>, 2015.
- Appleby, P. G. and Oldfield, F.: The calculation of lead-210 dates assuming a constant rate of supply of unsupported ²¹⁰Pb to the sediment, *Catena*, 5, 1–8, 1978.
- Barnes, P. W., Rearick, D. M., and Reimnitz, E.: Ice gouging characteristics and processes, in: *The Alaskan Beaufort Sea: Ecosystems and Environments*, 1st ed., edited by: Barnes, P. W., Schell, D. M., and Reimnitz, E., Academic Press, Orlando, Florida, USA, 185–212, 1984.
- Barnhart, K. R., Anderson, R. S., Overeem, I., Wobus, C., Clow, G. D., and Urban, F. E.: Modeling erosion of ice-rich permafrost bluffs along the Alaskan Beaufort Sea coast, *J. Geophys. Res. Earth Surf.*, 119, 1155–1179, <https://doi.org/10.1002/2013JF002845>, 2014.
- Baskaran, M., Bianchi, T. S., and Filley, T. R.: Inconsistencies between ¹⁴C and short-lived radionuclides-based sediment accumulation rates?: Effects of long-term remineralization, *J. Environ. Radioact.*, 174, 10–16, <https://doi.org/10.1016/j.jenvrad.2016.07.028>, 2017..
- Bauch, H. A., Kassens, H., Naidina, O. D., Kunz-Pirrung, M., and Thiede, J.: Composition and Flux of Holocene Sediments on the Eastern Laptev Sea Shelf, Arctic Siberia, *Quat. Res.*, 55, 344–351, <https://doi.org/10.1006/qres.2000.2223>, 2001a.
- Bauch, H. A., Mueller-Lupp, T., Taldenkova, E., Spielhagen, R. F., Kassens, H., Grootes, P. M., Thiede, J., Heinemeier, J., and Petryashov, V. V.: Chronology of the holocene transgression at the north siberian margin, *Glob. Planet. Change*, 31, 125–139, [https://doi.org/10.1016/S0921-8181\(01\)00116-3](https://doi.org/10.1016/S0921-8181(01)00116-3), 2001b.
- Boudreau, B. P.: Is burial velocity a master parameter for bioturbation?, *Geochim. Cosmochim. Acta*, 58, 1243–1249, [https://doi.org/10.1016/0016-7037\(94\)90378-6](https://doi.org/10.1016/0016-7037(94)90378-6), 1994.
- Bröder, L., Tesi, T., Semiletov, I. P., and Gustafsson, Ö.: Fate of permafrost-released organic matter in the Laptev Sea: What is its lateral transport time along the transect from the Lena delta area to the deep sea of the Arctic interior?, AGU Fall Meeting, San Francisco, USA, 14–18 December 2015, C33F-06, 2015.
- Bröder, L., Tesi, T., Andersson, A., Eglinton, T. I., Semiletov, I. P., Dudarev, O. V., Roos, P., and Gustafsson, Ö.: Historical records of organic matter supply and degradation status in the East Siberian Sea, *Org. Geochem.*, 91, 16–30, <https://doi.org/10.1016/j.orggeochem.2015.10.008>, 2016a.
- Bröder, L., Tesi, T., Salvadó, J. A., Semiletov, I. P., Dudarev, O. V., and Gustafsson, Ö.: Fate of terrigenous organic matter across the Laptev Sea from the mouth of the Lena River to the deep sea of the Arctic interior, *Biogeosciences*, 13, 5003–5019, <https://doi.org/10.5194/bg-13-5003-2016>, 2016b.
- Canuel, E. A. and Martens, C. S.: Reactivity of recently deposited organic matter?: near the sediment-water Degradation interface of lipid compounds, *Geochim. Cosmochim. Acta*, 60, 1793–1806, 1996.
- Ciais, P., Gasser, T., Paris, J. D., Caldeira, K., Raupach, M. R., Canadell, J. G., Patwardhan, A., Friedlingstein, P., Piao, S. L., and Gitz, V.: Attributing the increase in atmospheric CO₂ to emitters and absorbers, *Nat. Clim. Chang.*, 3, 926–930, <https://doi.org/10.1038/nclimate1942>, 2013.
- Conlan, K. E., Lenihan, H. S., Kvitek, R. G., and Oliver, J. S.: Ice scour disturbance to benthic communities in the Canadian High Arctic, *Mar. Ecol. Prog. Ser.*, 166, 1–16, <https://doi.org/10.3354/meps166001>, 1998.

- Crichton, K. A., Bouttes, N., Roche, D. M., Chappellaz, J., and Krinner, G.: Permafrost carbon as a missing link to explain CO₂ changes during the last deglaciation, *Nat. Geosci.*, 9, 683–686, <https://doi.org/10.1038/ngeo2793>, 2016.
- Cronin, T. M., O'Regan, M., Pearce, C., Gemery, L., Toomey, M., Semiletov, I., and Jakobsson, M.: Deglacial sea level history of the East Siberian Sea and Chukchi Sea margins, *Clim. Past*, 13, 1097–1110, <https://doi.org/10.5194/cp-13-1097-2017>, 2017.
- Elmqvist, M., Zencak, Z., and Gustafsson, Ö.: A 700 year sediment record of black carbon and polycyclic aromatic hydrocarbons near the EMEP air monitoring station in Aspöreten, Sweden, *Environ. Sci. Technol.*, 41, 6926–6932, <https://doi.org/10.1021/es070546m>, 2007.
- Farella, N., Lucotte, M., Louchouart, P., and Roulet, M.: Deforestation modifying terrestrial organic transport's, Brazilian Amazon in the Rio Tapajo, *Org. Geochem.*, 32, 1443–1458, 2001.
- Fisher, D., Dyke, A., Koerner, R., Bourgeois, J., Kinnard, C., Zdanowicz, C., de Vernal, A., Hillaire-Marcel, C., Savelle, J., and Rochon, A.: Natural Variability of Arctic Sea Ice Over the Holocene, *Eos, Trans. Am. Geophys. Union*, 87, 273–275, 2006.
- Fry, B. and Sherr, E. B.: $\delta^{13}\text{C}$ Measurements as indicators of carbon flow in marine and freshwater ecosystems, *Contrib. Mar. Sci.*, 27, 13–49, 1984.
- Goñi, M. A. and Hedges, J. I.: Sources and reactivities of marine-derived organic matter in coastal sediments as determined by alkaline CuO oxidation, *Geochim. Cosmochim. Acta*, 59, 2965–2981, [https://doi.org/10.1016/0016-7037\(95\)00188-3](https://doi.org/10.1016/0016-7037(95)00188-3), 1995.
- Goñi, M. A. and Montgomery, S.: Alkaline CuO oxidation with a microwave digestion system: Lignin analyses of geochemical samples, *Anal. Chem.*, 72, 3116–3121, <https://doi.org/10.1021/ac991316w>, 2000.
- Goñi, M. A., Yunker, M. B., MacDonald, R. W., and Eglinton, T. I.: Distribution and sources of organic biomarkers in arctic sediments from the Mackenzie River and Beaufort Shelf, *Mar. Chem.*, 71, 23–51, [https://doi.org/10.1016/S0304-4203\(00\)00037-2](https://doi.org/10.1016/S0304-4203(00)00037-2), 2000.
- Goñi, M. A., O'Connor, A. E., Kuzyk, Z. Z., Yunker, M. B., Gobeil, C., and Macdonald, R. W.: Distribution and sources of organic matter in surface marine sediments across the North American Arctic margin, *J. Geophys. Res. Ocean.*, 118, 4017–4035, <https://doi.org/10.1002/jgrc.20286>, 2013.
- Gordeev, V. V.: Fluvial sediment flux to the Arctic Ocean, *Geomorphology*, 80, 94–104, <https://doi.org/10.1016/j.geomorph.2005.09.008>, 2006.
- Grigoriev, M.: Coastal sediment and organic carbon flux to the Laptev and East Siberian Seas, EGU General Assembly Conference Abstracts, 12, 8763, 2010.
- Grigoriev, M. N. and Rachold, V.: The degradation of coastal permafrost and the organic carbon balance of the Laptev and East Siberian Seas, *Permafrost. Proc. 8th Int. Conf. Permafrost*, 21–25 July 2003, Zurich, Switz. (1987), 319–324, 2003.
- Günther, F., Overduin, P. P., Yakshina, I. A., Opel, T., Baranskaya, A. V., and Grigoriev, M. N.: Observing Muostakh disappear: permafrost thaw subsidence and erosion of a ground-ice-rich island in response to arctic summer warming and sea ice reduction, *The Cryosphere*, 9, 151–178, <https://doi.org/10.5194/tc-9-151-2015>, 2015.
- Hartnett, H., Keil, R., Hedges, J., and Devol, A.: Influence of oxygen exposure time on organic carbon preservation in continental margin sediments, *Nature*, 391, 572–575, <https://doi.org/10.1038/35351>, 1998.
- Hedges, J. I., Blanchette, R. A., Weliky, K., and Devol, A. H.: Effects of fungal degradation on the CuO oxidation products of lignin: A controlled laboratory study, *Geochim. Cosmochim. Acta*, 52, 2717–2726, [https://doi.org/10.1016/0016-7037\(88\)90040-3](https://doi.org/10.1016/0016-7037(88)90040-3), 1988.
- Higuchi, T.: Formation and biological degradation of lignins, *Adv. Enzym. Relat. Areas. Mol. Biol.*, 34, 207–283, 1971.
- Hilton, R. G., Galy, V., Gaillardet, J., Dellinger, M., Bryant, C., O'Regan, M., Gröcke, D. R., Coxall, H., Bouchez, J., and Calmels, D.: Erosion of organic carbon in the Arctic as a geological carbon dioxide sink, *Nature*, 524, 84–87, <https://doi.org/10.1038/nature14653>, 2015.
- Hugelius, G., Strauss, J., Zubrzycki, S., Harden, J. W., Schuur, E. A. G., Ping, C.-L., Schirmer, L., Grosse, G., Michaelson, G. J., Koven, C. D., O'Donnell, J. A., Elberling, B., Mishra, U., Camill, P., Yu, Z., Palmtag, J., and Kuhry, P.: Estimated stocks of circumpolar permafrost carbon with quantified uncertainty ranges and identified data gaps, *Biogeosciences*, 11, 6573–6593, <https://doi.org/10.5194/bg-11-6573-2014>, 2014.
- IPCC Working Group I, I., Stocker, T. F., Qin, D., Plattner, G.-K., Tignor, M., Allen, S. K., Boschung, J., Nauels, A., Xia, Y., Bex, V., and Midgley, P. M.: IPCC, 2013: Climate Change 2013: The Physical Science Basis, Contribution of Working Group I to the Fifth Assessment Report of the Intergovernmental Panel on Climate Change, IPCC, AR5, 1535, 2013.
- Jakobsson, M.: Hypsometry and volume of the Arctic Ocean and its constituent seas, *Geochem. Geophys. Geosystems*, 3, 1–18, 2002.
- Jakobsson, M., Andreassen, K., Bjarnadóttir, L. R., Dove, D., Dowdeswell, J. A., England, J. H., Funder, S., Hogan, K., Ingólfsson, Ó., Jennings, A., Krog Larsen, N., Kirchner, N., Landvik, J. Y., Mayer, L., Mikkelsen, N., Möller, P., Niessen, F., Nilsson, J., O'Regan, M., Polyak, L., Nørgaard-Pedersen, N., and Stein, R.: Arctic Ocean glacial history, *Quat. Sci. Rev.*, 92, 40–67, <https://doi.org/10.1016/j.quascirev.2013.07.033>, 2014.
- Jones, B. M., Arp, C. D., Jorgenson, M. T., Hinkel, K. M., Schmutz, J. A., and Flint, P. L.: Increase in the rate and uniformity of coastline erosion in Arctic Alaska, *Geophys. Res. Lett.*, 36, 1–5, <https://doi.org/10.1029/2008GL036205>, 2009.
- Kanevskiy, M., Shur, Y., Strauss, J., Jorgenson, T., Fortier, D., Stephani, E., and Vasiliev, A.: Patterns and rates of riverbank erosion involving ice-rich permafrost (yedoma) in northern Alaska, *Geomorphology*, 253, 370–384, <https://doi.org/10.1016/j.geomorph.2015.10.023>, 2016.
- Karlsson, E. S., Charkin, A., Dudarev, O., Semiletov, I., Vonk, J. E., Sánchez-García, L., Andersson, A., and Gustafsson, Ö.: Carbon isotopes and lipid biomarker investigation of sources, transport and degradation of terrestrial organic matter in the Buor-Khaya Bay, SE Laptev Sea, *Biogeosciences*, 8, 1865–1879, <https://doi.org/10.5194/bg-8-1865-2011>, 2011.
- Karlsson, E. S., Brüchert, V., Tesi, T., Charkin, A., Dudarev, O., Semiletov, I., and Gustafsson, O.: Contrasting regimes for organic matter degradation in the East Siberian Sea and the Laptev Sea assessed through microbial incubations and molecular markers, *Mar. Chem.*, 170, 11–22, <https://doi.org/10.1016/j.marchem.2014.12.005>, 2015.

- Karllsson, E. S., Gelting, J., Tesi, T., Dongen, B., Andersson, A., Semiletov, I., Charkin, A., Dudarev, O., and Gustafsson, Ö.: Different sources and degradation state of dissolved, particulate, and sedimentary organic matter along the Eurasian Arctic coastal margin, *Global Biogeochem. Cycles*, 30, 898–919, <https://doi.org/10.1002/2015GB005307>, 2016.
- Kaufman, D. S., Ager, T. A., Anderson, N. J., Anderson, P. M., Andrews, J. T., Bartlein, P. J., Brubaker, L. B., Coats, L. L., Cwynar, L. C., Duvall, M. L., Dyke, A. S., Edwards, M. E., Eisner, W. R., Gajewski, K., Geirsdóttir, A., Hu, F. S., Jennings, A. E., Kaplan, M. R., Kerwin, M. W., Lozhkin, A. V., MacDonald, G. M., Miller, G. H., Mock, C. J., Oswald, W. W., Otto-Bliesner, B. L., Porinchu, D. F., Rühland, K., Smol, J. P., Steig, E. J. and Wolfe, B. B.: Holocene thermal maximum in the western Arctic (0–180° W), *Quat. Sci. Rev.*, 23, 529–560, <https://doi.org/10.1016/j.quascirev.2003.09.007>, 2004.
- Keil, R. G., Dickens, A. F., Arnarson, T., Nunn, B. L., and Devol, A. H.: What is the oxygen exposure time of laterally transported organic matter along the Washington margin?, *Mar. Chem.*, 92, 157–165, <https://doi.org/10.1016/j.marchem.2004.06.024>, 2004.
- Kohlbach, D., Graeve, M., A. Lange, B., David, C., Peeken, I., and Flores, H.: The importance of ice algae-produced carbon in the central Arctic Ocean ecosystem: Food web relationships revealed by lipid and stable isotope analyses, *Limnol. Oceanogr.*, 61, 2027–2044, <https://doi.org/10.1002/lno.10351>, 2016.
- Köhler, P., Knorr, G., and Bard, E.: Permafrost thawing as a possible source of abrupt carbon release at the onset of the Bølling/Allerød, *Nature Communications*, 5, 5520, <https://doi.org/10.1038/ncomms6520>, 2014.
- Koven, C. D., Ringeval, B., Friedlingstein, P., Ciais, P., Cadule, P., Khvorostyanov, D., Krinner, G., and Tarnocai, C.: Permafrost carbon-climate feedbacks accelerate global warming, *Proc. Natl. Acad. Sci.*, 108, 14769–14774, <https://doi.org/10.1073/pnas.1103910108>, 2011.
- Kunst, L. and Samuels, A. L.: Biosynthesis and secretion of plant cuticular wax, *Prog. Lipid Res.*, 42, 51–80, [https://doi.org/10.1016/S0163-7827\(02\)00045-0](https://doi.org/10.1016/S0163-7827(02)00045-0), 2003.
- Lambeck, K., Rouby, H., Purcell, A., Sun, Y., and Sambridge, M.: Sea level and global ice volumes from the Last Glacial Maximum to the Holocene, *Proc. Natl. Acad. Sci.*, 111, 15296–15303, <https://doi.org/10.1073/pnas.1411762111>, 2014.
- Louchouart, P., Lucotte, M., and Farella, N.: Historical and geographical variations of sources and transport of terrigenous organic matter within a large-scale coastal environment, *Org. Geochem.*, 30, 675–699, [https://doi.org/10.1016/S0146-6380\(99\)00019-4](https://doi.org/10.1016/S0146-6380(99)00019-4), 1999.
- McClelland, J. W., Holmes, R. M., Peterson, B. J., Raymond, P. A., Striegl, R. G., Zhulidov, A. V., Zimov, S. A., Zimov, N., Tank, S. E., Spencer, R. G. M., Staples, R., Gurtovaya, T. Y., and Griffin, C. G.: Particulate organic carbon and nitrogen export from major Arctic rivers, *Global Biogeochem. Cycles*, 30, 629–643, <https://doi.org/10.1002/2015GB005351>, 2016.
- Mueller-Lupp, T., Bauch, H. A., Erlenkeuser, H., Hefter, J., Kassens, H., and Thiede, J.: Changes in the deposition of terrestrial organic matter on the Laptev Sea shelf during the Holocene: evidence from stable carbon isotopes, *Int. J. Earth Sci.*, 89, 563–568, <https://doi.org/10.1007/s005310000128>, 2000.
- Olefeldt, D., Goswami, S., Grosse, G., Hayes, D., Hugelius, G., Kuhry, P., McGuire, A. D., Romanovsky, V. E., Sannel, A. B. K., Schuur, E. A. G., and Turetsky, M. R.: Circumpolar distribution and carbon storage of thermokarst landscapes, *Nat. Commun.*, 7, 13043, <https://doi.org/10.1038/ncomms13043>, 2016.
- Opsahl, S. and Benner, R.: Early diagenesis of vascular plant tissues: Lignin and cutin decomposition and biogeochemical implications, *Geochim. Cosmochim. Acta*, 59, 4889–4904, [https://doi.org/10.1016/0016-7037\(95\)00348-7](https://doi.org/10.1016/0016-7037(95)00348-7), 1995.
- Parnell, A. C., Phillips, D. L., Bearhop, S., Semmens, B. X., Ward, E. J., Moore, J. W., Jackson, A. L., Grey, J., Kelly, D. J., and Inger, R.: Bayesian stable isotope mixing models, *Environmetrics*, 24, 387–399, <https://doi.org/10.1002/env.2221>, 2013.
- Pearson, A., McNichol, A. P., Schneider, R. J., Von Reden, K. F., and Zheng, Y.: Microscale AMS 14C measurements at NOSAMS, *Radiocarbon*, 40, 61–75, 1998.
- Prahl, F. G., Ertel, J. R., Goni, M. A., Sparrow, M. A., and Eversmeyer, B.: Terrestrial organic carbon contributions to sediments on the Washington margin, *Geochim. Cosmochim. Acta*, 58, 3035–3048, [https://doi.org/10.1016/0016-7037\(94\)90177-5](https://doi.org/10.1016/0016-7037(94)90177-5), 1994.
- Ramsey, C. B.: Deposition models for chronological records, *Quat. Sci. Rev.*, 27, 42–60, <https://doi.org/10.1016/j.quascirev.2007.01.019>, 2008.
- Ramsey, C. B. and Lee, S.: Recent and Planned Developments of the Program OxCal, *Radiocarbon*, 55, 720–730, <https://doi.org/10.1017/S0033822200057878>, 2013.
- Reimer, P. J., Bard, E., Bayliss, A., Beck, J. W., Blackwell, P. G., Ramsey, C. B., Buck, C. E., Cheng, H., Edwards, R. L., Friedrich, M., Grootes, P. M., Guilderson, T. P., Haflidason, H., Hajdas, I., Hatté, C., Heaton, T. J., Hoffmann, D. L., Hogg, A. G., Hughen, K. A., Kaiser, K. F., Kromer, B., Manning, S. W., Niu, M., Reimer, R. W., Richards, D. A., Scott, E. M., Southon, J. R., Staff, R. A., Turney, C. S. M., and van der Plicht, J.: IntCal13 and Marine13 Radiocarbon Age Calibration Curves 0–50000 Years cal BP, *Radiocarbon*, 55, 1869–1887, https://doi.org/10.2458/azu_js_rc.55.16947, 2013.
- Romanovskii, N. N., Hubberten, H. W., Gavrillov, A. V., Tumskoy, V. E., and Kholodov, A. L.: Permafrost of the east Siberian Arctic shelf and coastal lowlands, *Quat. Sci. Rev.*, 23, 1359–1369, <https://doi.org/10.1016/j.quascirev.2003.12.014>, 2004.
- Salvadó, J. A., Tesi, T., Sundbom, M., Karlsson, E., Kruså, M., Semiletov, I. P., Panova, E., and Gustafsson, Ö.: Contrasting composition of terrigenous organic matter in the dissolved, particulate and sedimentary organic carbon pools on the outer East Siberian Arctic Shelf, *Biogeosciences*, 13, 6121–6138, <https://doi.org/10.5194/bg-13-6121-2016>, 2016.
- Sánchez-García, L., Alling, V., Pugach, S., Vonk, J., Van Dongen, B., Humborg, C., Dudarev, O., Semiletov, I., and Gustafsson, Ö.: Inventories and behavior of particulate organic carbon in the Laptev and East Siberian seas, *Global Biogeochem. Cycles*, 25, 1–13, <https://doi.org/10.1029/2010GB003862>, 2011.
- Schirmer, L., Kunitsky, V., Grosse, G., Wetterich, S., Meyer, H., Schwaborn, G., Babiy, O., Derevyagin, A., and Siegert, C.: Sedimentary characteristics and origin of the Late Pleistocene Ice Complex on north-east Siberian Arctic coastal lowlands and islands – A review, *Quat. Int.*, 241, 3–25, <https://doi.org/10.1016/j.quaint.2010.04.004>, 2011.
- Schlitzer, R.: Ocean Data View, available at: <http://odv.awi.de> (last access: 8 December 2016), 2015.

- Schuur, E. A. G., McGuire, A. D., Schädel, C., Grosse, G., Harden, J. W., Hayes, D. J., Hugelius, G., Koven, C. D., Kuhry, P., Lawrence, D. M., Natali, S. M., Olefeldt, D., Romanovsky, V. E., Schaefer, K., Turetsky, M. R., Treat, C. C., and Vonk, J. E.: Climate change and the permafrost carbon feedback, *Nature*, 520, 171–179, <https://doi.org/10.1038/nature14338>, 2015.
- Semiletov, I. P.: Aquatic Sources and Sinks of CO₂ and CH₄ in the Polar Regions, *J. Atmos. Sci.*, 56, 286–306, 1999a.
- Semiletov, I. P.: Destruction of the coastal permafrost ground as an important factor in biogeochemistry of the Arctic Shelf waters, *Trans. [Doklady] Russ. Acad. Sci.*, 368, 679–682, 1999b.
- Semiletov, I. P., Dudarev, O., Luchin, V., Charkin, A., Shin, K. H., and Tanaka, N.: The East Siberian Sea as a transition zone between Pacific-derived waters and Arctic shelf waters, *Geophys. Res. Lett.*, 32, 1–5, <https://doi.org/10.1029/2005GL022490>, 2005.
- Semiletov, I. P., Shakhova, N. E., Pipko, I. I., Pugach, S. P., Charkin, A. N., Dudarev, O. V., Kosmach, D. A., and Nishino, S.: Space-time dynamics of carbon and environmental parameters related to carbon dioxide emissions in the Buor-Khaya Bay and adjacent part of the Laptev Sea, *Biogeosciences*, 10, 5977–5996, <https://doi.org/10.5194/bg-10-5977-2013>, 2013.
- Smith, S. L., Henrichs, S. M., and Rho, T.: Stable C and N isotopic composition of sinking particles and zooplankton over the southeastern Bering Sea shelf, *Deep. Res. Part II Top. Stud. Oceanogr.*, 49, 6031–6050, 2002.
- Stanford, J. D., Hemingway, R., Rohling, E. J., Challenor, P. G., Medina-elizalde, M., and Lester, A. J.: Sea-level probability for the last deglaciation?: A statistical analysis of far-field records, *Glob. Planet. Change*, 79, 193–203, <https://doi.org/10.1016/j.gloplacha.2010.11.002>, 2011.
- Stein, R. and Macdonald, R. W. (Eds.): *The organic carbon cycle in the Arctic Ocean*, Springer-Verlag, Berlin, Heidelberg, Germany, 2004.
- Stuiver, M. and Braziunas, T. F.: Modeling Atmospheric ¹⁴C Influences and ¹⁴C Ages of Marine Samples to 10,000 BC, *Radiocarbon*, 35, 137–189, <https://doi.org/10.1017/S0033822200013874>, 1993.
- Stuiver, M. and Polach, H. A.: Radiocarbon, *Radiocarbon*, 19, 355–363, <https://doi.org/10.1021/ac100494m>, 1977.
- Tamocai, C., Canadell, J. G., Schuur, E. A. G., Kuhry, P., Mazhitova, G., and Zimov, S.: Soil organic carbon pools in the northern circumpolar permafrost region, *Global Biogeochem. Cycles*, 23, 1–11, <https://doi.org/10.1029/2008GB003327>, 2009.
- Tesi, T., Semiletov, I., Hugelius, G., Dudarev, O., Kuhry, P., and Gustafsson, Ö.: Composition and fate of terrigenous organic matter along the Arctic land-ocean continuum in East Siberia: Insights from biomarkers and carbon isotopes, *Geochim. Cosmochim. Acta*, 133, 235–256, <https://doi.org/10.1016/j.gca.2014.02.045>, 2014.
- Tesi, T., Muschitiello, F., Smittenberg, R. H., Jakobsson, M., Vonk, J. E., Hill, P., Andersson, A., Kirchner, N., Noormets, R., Dudarev, O., Semiletov, I., and Gustafsson, Ö.: Massive remobilization of permafrost carbon during post-glacial warming, *Nat. Commun.*, 7, 13653, <https://doi.org/10.1038/ncomms13653>, 2016a.
- Tesi, T., Semiletov, I., Dudarev, O., Andersson, A., and Gustafsson, Ö.: Matrix association effects on hydrodynamic sorting and degradation of terrestrial organic matter during cross-shelf transport in the Laptev and East Siberian shelf seas, *J. Geophys. Res.-Biogeosci.*, 121, 731–752, <https://doi.org/10.1002/2015JG003067>, 2016b.
- Vetrov, A. and Romankevich, E. (Eds.): *Carbon Cycle in the Russian Arctic Seas*, 1st ed., Springer-Verlag, Berlin, Heidelberg, Germany, 2004.
- Vonk, J. E. and Gustafsson, Ö.: Permafrost-carbon complexities, *Nat. Geosci.*, 6, 675–676, <https://doi.org/10.1038/ngeo1937>, 2013.
- Vonk, J. E., Sánchez-García, L., Semiletov, I., Dudarev, O., Eglinton, T., Andersson, A., and Gustafsson, Ö.: Molecular and radiocarbon constraints on sources and degradation of terrestrial organic carbon along the Kolyma paleoriver transect, East Siberian Sea, *Biogeosciences*, 7, 3153–3166, <https://doi.org/10.5194/bg-7-3153-2010>, 2010.
- Vonk, J. E., Sánchez-García, L., van Dongen, B. E., Alling, V., Kosmach, D., Charkin, A., Semiletov, I. P., Dudarev, O. V., Shakhova, N., Roos, P., Eglinton, T. I., Andersson, A., and Gustafsson, Ö.: Activation of old carbon by erosion of coastal and subsea permafrost in Arctic Siberia, *Nature*, 489, 137–140, <https://doi.org/10.1038/nature11392>, 2012.
- Winterfeld, M., Goñi, M. A., Just, J., Hefter, J., and Mollenhauer, G.: Characterization of particulate organic matter in the Lena River delta and adjacent nearshore zone, NE Siberia – Part 2: Lignin-derived phenol compositions, *Biogeosciences*, 12, 2261–2283, <https://doi.org/10.5194/bg-12-2261-2015>, 2015.